



Interpretation of pipe-jacking and lubrication records for drives in silty soil

Kevin G. O'Dwyer^a, Bryan A. McCabe^{a,*}, Brian B. Sheil^b

^a Civil Engineering, College of Engineering and Informatics, National University of Ireland, Galway, Ireland

^b Department of Engineering Science, University of Oxford, United Kingdom

Received 14 November 2018; received in revised form 22 February 2019; accepted 7 April 2019

Available online 22 April 2019

Abstract

In recent years, there has been an increased resort to microtunnelling/pipe-jacking as a means of constructing underground conduits (for water, sewage, gas, and other utilities) to avoid on-street disruption in urban areas. In this paper, technical details of two 1200 mm internal diameter microtunnels in silty sand totalling over 550 m in length are discussed. While average skin friction values are extremely low for both drives suggesting effective lubrication practice, differences in normalised bentonite volumes appear to be responsible for differences in skin friction. Full or near full buoyancy of the pipeline has been demonstrated for the majority of the drive. The frictional stress increase after a stoppage is shown to depend on not only the stoppage duration but also on the normalised lubrication volume. Interpretation of data in the manner presented in the paper is an important means of assimilating experience of microtunnelling in different ground conditions.

Keywords: Microtunnelling; Pipe-jacking; Skin friction; Lubrication; Pipe buoyancy; Stoppages

1 Introduction

Rapid urbanization worldwide has resulted in an escalating need to provide new and upgrade existing water, sewage, gas/oil, electricity and other utility conveyance networks. Microtunnelling or pipe-jacking has emerged as the preferred method of utility pipeline construction, as it avoids the on-street disruption associated with trenches constructed from the ground surface. However, the difficulty in identifying suitable intermediate shaft locations in built-up areas means that long tunnel drives are often necessary; maintaining jacking forces at manageable levels can be a challenge in these drives. For example, excessive stress concentrations can give rise to spalling at the joints between pipes, with the potential to induce pipe failure (Chapman & Ichioka, 1999; Zhang, Behbahani, Ma,

Iseley, & Tan, 2018). Intermediate jacking stations (i.e. installed within the tunnel) are sometimes used, but are cumbersome and expensive and therefore avoided where possible.

The total jacking force (F_{total}) consists of the force at the face (F_{face}) of the tunnel boring machine (TBM) and the frictional force (F_{friction}) between the string elements (TBM, powerpack, can and pipe train) and the surrounding ground. F_{friction} is often the main contribution to F_{total} , especially in long drives (Cheng, Ni, Shen, & Huang, 2017). The average skin friction for a drive can be calculated as F_{friction} divided by the embedded surface area of all elements. However, the skin friction (τ) associated with the pipes (comprising the majority of the string length) is of greater interest, and is calculated as the portion of F_{friction} associated with the pipe string divided by the embedded surface area of the pipe string. This value of τ depends on the normal effective stress (σ'_n) from the soil on the pipes, the effective weight (W_{eff}) of the pipes, i.e. weight

* Corresponding author.

E-mail address: bryan.mccabe@nuigalway.ie (B.A. McCabe).

minus buoyant force (weight taken as positive downwards), and the angle of effective interface shearing resistance between the pipes and the ground, δ_p :

$$\tau = \left(\sigma'_n + \frac{|W_{\text{eff}}|}{\pi DL} \right) \tan \delta_p, \quad (1)$$

where D is the external pipe diameter, and L is the pipe string length.

The introduction of a lubricant into the overcut (the annulus formed on account of the TBM having a larger diameter than the pipes) is well known to be an effective means of reducing τ (e.g. Marshall, 1998; Chapman & Ichioka, 1999; Borghi, 2006; Shou, Yen, & Liu, 2010; McGillivray & Frost, 2010; Barla & Camusso, 2013). In the context of Eq. (1), there are two scenarios to consider:

- (1) *Stable overcut*: If the pipe string is buoyant in the lubricant, W_{eff} will be lower than the weight of the pipe W , and may be negative (i.e. net upwards force). The ideal scenario is when the pipe is centred within the bore, in which case the normal effective stress (σ'_n) is zero. In practice, ballast can be used to enable the pipe string to achieve this position (Praetorius & Schöber, 2017). Any contact between the pipe and the bore will generate a normal effective stress. The value of δ_p of a lubricant-pipe interface will be lower than that of a soil-pipe interface.
- (2) *Unstable overcut*: Buoyancy may still occur (i.e. $W_{\text{eff}} < W$), but to a lesser extent than in (1) due to the higher specific gravity of the lubricant-soil mixture. An arching mechanism, originally identified by Terzaghi (1943), governs the normal effective stress on the pipe. Staheli (2006) suggested that it may be appropriate to assume that a uniform normal effective stress σ'_n of the same magnitude as the vertical effective stress σ'_v acts perpendicularly to the pipeline for the full pipeline circumference; Reilly (2014) has deemed this to be acceptable through numerical modelling. Methods of calculating σ'_v are considered in Section 3.4. Finally, the value of δ_p at the interface between the lubricant-soil mixture and the pipe will be lower than that of an unlubricated soil-pipe interface.

In practice, there remains considerable uncertainty over whether the overcut remains stable in certain ground

conditions and the values of σ'_n , W_{eff} and δ_p in existence as a consequence.

Low average τ values over the course of a drive are readily achievable, especially in a stable lubricated overcut. Values for silt are scarce in the literature; a selection of values for sand drives is shown in Table 1. Values as low as 0.1 kPa have been reported by Cheng, Ni, Arulrajah, and Huang (2018). However, it is the increased forces encountered upon resumption of jacking after stoppages that typically govern jacking force requirements. This increase is a result of the elevation in frictional resistance at a constant value of face resistance (Cheng et al., 2017). Chapman and Ichioka (1999) considered that there was potential for bentonite consolidation during longer stoppages such as nights and weekends. Alternatively, Zhang et al. (2018) suggested that the jacking force increase may be a consequence of bentonite pressure reduction in the annulus during a stoppage, leading to cavity contraction, thereby increasing the effective soil pressure acting on the concrete pipes. The same authors also inferred differences in the coefficients of static and dynamic friction. Jacking force increases in coarse soils have been quantified by a number of authors:

- (1) Pellet-Beaucour and Kastner (2002) reported additional skin friction values of 0.6–0.8 kPa for stoppages less than 3 h and 1.1–2.0 kPa for overnight stoppages in sand/silt sites.
- (2) Curran and McCabe (2011) found that the stoppage duration had an effect on the jacking force increase in clay but not in a dense sandy gravel. In the latter case, a further 0.8 kPa had to be overcome for a short stoppage (<1.5 h) and an additional 0.84 kPa for a long stoppage (>12 h).
- (3) Cheng et al. (2017) reported that a ‘short’ stoppage required an additional 0.52 kPa to be overcome, while ‘long’ stoppages required an increase of 1.0 kPa for drives in a poorly-graded gravel or sand deposit.
- (4) Zhang et al. (2018) observed increases in jacking force between 0.1 kPa for stoppages less than 2 h and 2.16 kPa for stoppages longer than 20 h.

Clearly these findings are not entirely consistent, so there is scope for further research on the effect of stoppages on jacking forces.

Herrenknecht slurry-shield microtunnelling machines and volume-controlled bentonite lubrication systems

Table 1
Selected skin friction values reported in sand.

Lubricated?	Ground conditions	Skin friction (kPa)	Reference
No	Sand	2.8–4.0	Pellet-Beaucour and Kastner (2002)
Yes	Dense sand	2.6	Curran and McCabe (2011)
Yes	Sand	0.5–2.5	Reilly and Orr (2012)
Yes	Gravelly coarse sand	0.32–4.46	Zhang et al. (2018)
Yes	Fine soil governed gravel or sand deposit	0.09	Cheng et al. (2018)

(Ulkan, 2013) are commonly used in pipe-jacking contracts. A large number of parameters are recorded at regular time/distance intervals from both the tunnelling and lubrication processes, but rarely are any retrospective analyses carried out on these data. In this paper, data from two drives on a U.K. pipe-jacking project are analysed to provide insight into some of the knowledge gaps identified above.

2 Pipe-jacking project and tunnelling details

2.1 Project

The Blackpool South Strategy Project was devised to improve bathing water quality along the Blackpool (U.K.) seafront and mitigate the risk of flooding after periods of heavy rainfall. One component of this scheme entailed the construction of a new storm-water holding tank at Lennox Gate and a tunnel to accommodate 700 mm internal diameter ductile water pipes connecting the holding tank to an outfall at Harrowside, from where the water is fed to the sea. The tunnels were constructed by Ward and Burke Construction Ltd. Tunnelling and lubrication data from the two drives (A and B) shown in Fig. 1 are considered in this paper.

2.2 Drive details

Drive A was 272 m in length, constructed in an east north-easterly direction with a gradient of -0.154% and an initial launch invert depth of 7.61 m. Drive B was 295 m in length, constructed in a west south-westerly direction with a gradient of 0.347% and an initial launch invert depth of 7.59 m (Fig. 1). Cover depths ranged from 5.2–6.3 m for Drive A to 6.2–7.8 m for Drive B. The TBM used was a Herrenknecht AVN 1200 (slurry shield machine), with a cutterhead diameter of 1 515 mm and a machine lining outer diameter of 1 505 mm. Each concrete pipe was 2.5 m long with an outer diameter of 1 490 mm, providing

an overcut 25 mm thick, corresponding to an overcut ratio of 1.68%. The mass of each pipe was 3 660 kg.

2.3 Lubrication details

The lubrication used was a bentonite solution comprising Hydraul-EZ and water in the ratio 22.7 kg to 400 L (5.7%). Other additives included (1) soda ash to balance pH, (2) MX polymer to prevent additional groundwater penetrating the mix, and (3) torque reducer to promote lubrication. The first bentonite station was located in the pipe directly behind the TBM, with 19 further stations positioned in ensuing pipes (one every fifth pipe). Each of these stations comprised three lubrication ports, separated by 120° , situated mid-length on each pipe. One further bentonite station was fixed to the launch shaft wall. The bentonite system used was volume-controlled, calculated from the TBM advance rate and ground conditions (Ulkan, 2013).

2.4 Ground conditions

The locations of three boreholes (BH4, BH6, and BH8) in relation to the line of Drives A and B are shown in Fig. 1. The ground conditions comprise made ground (0.4 m thickness), underlain by gravelly sand (2.6–4.4 m), peat (1.0–1.7 m), silt (1.2–2.5 m) and silty sand/sand (>5.0 m). From the summary stratigraphy in Fig. 2, it can be seen that the tunnel passes through the silt and silty sand layers. The water table was found to be at a depth of 1.2 m in a borehole close to the reception shaft of Drive A.

Uncorrected Standard penetration test (SPT) values N are also shown in Fig. 2. In order to derive an operational friction angle for the material above the crown of the tunnel for stability assessments (Section 3.4), it was assumed that the material above the tunnel crown was predominantly granular (i.e. the peat was ignored). Therefore, an average N_1 value (N values corrected for overburden pressure) for the layer could be correlated with the friction

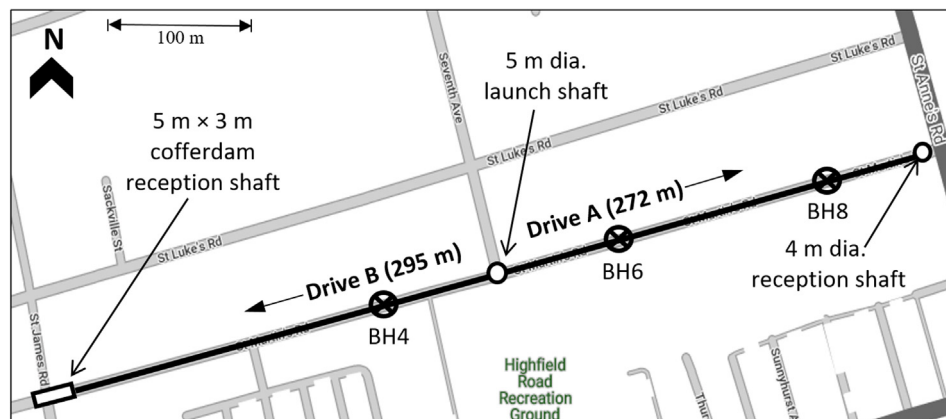


Fig. 1. Location of tunnels and shafts at Blackpool site (adapted from Google Maps).

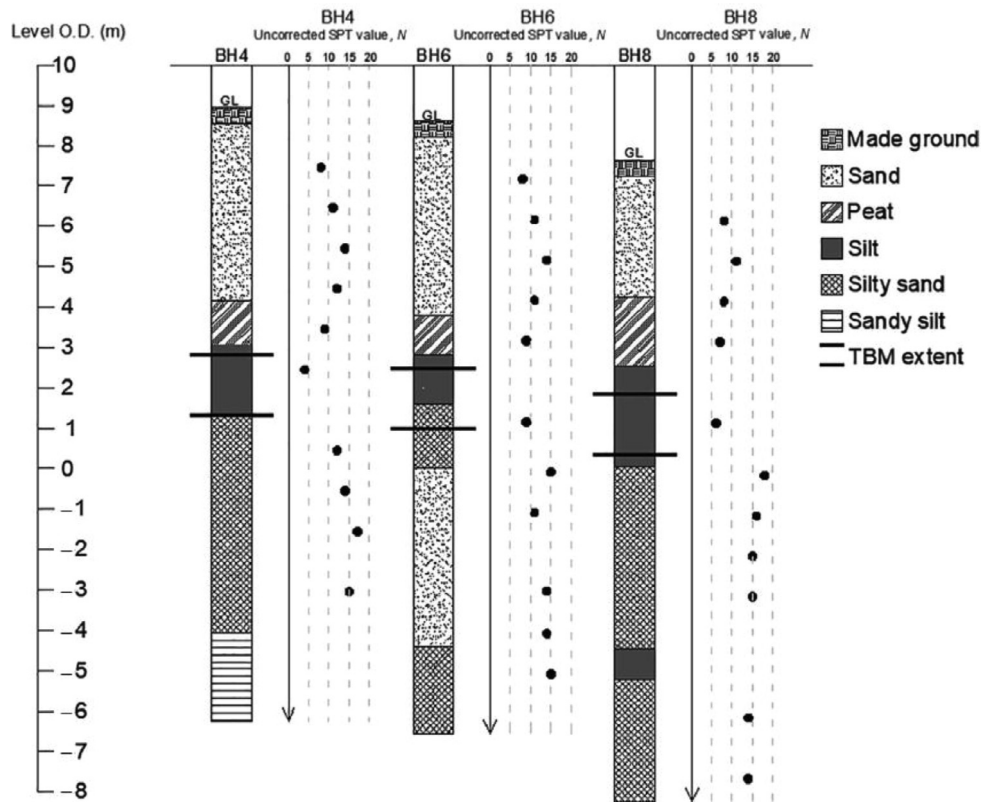


Fig. 2. Stratigraphy and uncorrected SPT profiles.

angle (Stroud, 1989). This exercise yielded a friction angle of approximately 32° .

3 Monitoring results and discussion

3.1 Jacking force

The output data from the TBM were recorded at 200 mm intervals of jacked distance. Due to a technical issue with the data acquisition system, data for Drive B

were only recorded beyond a jacked distance of 62 m. The developments of working pressure (a proxy for torque) and total jacking force (F_{total}) with jacked distance are shown in Figs. 3(a) (Drive A) and 3(b) (Drive B). The working pressure is relatively constant over the length of the drives, reflecting a consistent driving style. F_{total} increased marginally with jacked length (average values of 380 kN for Drive A and 430 kN for Drive B), but rose to over 1 000 kN near the end of the drive, as the TBM approached the concrete wall of the reception shaft.

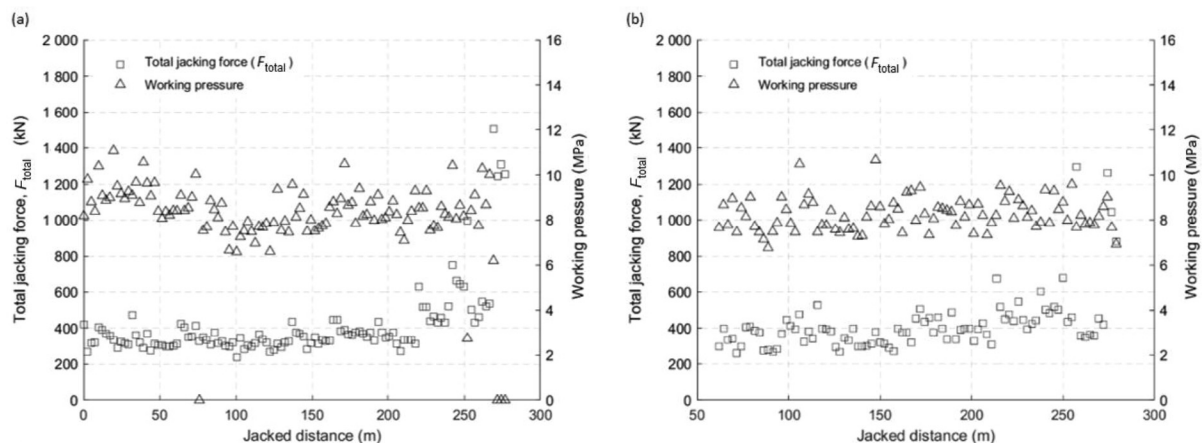


Fig. 3. Developments of total jacking force and working pressure during (a) Drive A and (b) Drive B.

F_{face} was not measured directly in this type of Herrenknecht machine, so the approach of Pellet-Beaucour and Kastner (2002) was typically used to separate F_{face} and F_{friction} (e.g. Curran & McCabe, 2011; Sheil, Curran, & McCabe, 2016; Ni, Ge, & Cheng, 2016; Cheng et al., 2018). F_{friction} could be approximated from a trendline joining the minimum points of a total jacking load versus jacked distance plot, while F_{face} was taken as the difference between the minimum and maximum envelopes. The sensitivity of F_{friction} to the intervals over which the minimum jacking forces were assessed was considered by calculating F_{friction} values over 1 m, 2.4 m (approximately one pipe length), 5 m and 10 m intervals. F_{friction} values were found to reduce with increased interval, converging to consistent values at 10 m intervals. Therefore, the F_{face} and F_{friction} values presented in Fig. 4 are based on the maximum and minimum forces over 10 m intervals.

The effectiveness of lubrication is best assessed from τ values for the pipe string only. The heavier elements (TBM, power pack and can) are likely to drag along the bottom of the overcut, generating much higher levels of friction than the pipes. It is also conceivable that there is a transition zone where the position of the pipes in the overcut is dictated by the heavier elements (illustrated in Fig. 5; stable overcut assumed for the purposes of figure). To this end, the frictional force for the first 62 m has been subtracted from the data; this distance was chosen as it coincides with the point at which data recording for Drive B commenced.

It can be seen from Fig. 6 that the τ values are at the low end of the range indicated in Table 1, suggesting effective lubrication practice. The skin friction values at any stage of Drive A are typically below 0.25 kPa, whereas those for Drive B are higher on average and typically below 0.5 kPa over the length of the drive. The small negative τ values plotted on Fig. 6 (mainly for Drive A) are believed to arise from small errors associated with the Pellet-Beaucour and Kastner (2002) force separation process superimposed on very low real skin friction values.

Large deviations in alignment, irrespective of the cause, can increase the required jacking force. Reilly, McCabe, and Orr (2012) reported on two drives of similar length and in similar ground conditions; at a jacked distance of 60 m, one drive deviated by 270 mm and required a jacking load of 3 750 kN at this point, whereas the other drive deviated by 137 mm and required a jacking load of 2 300 kN. From field monitoring of a drive in ground described as ‘fine soil governed gravel or sand deposit’, Cheng et al. (2018) suggested that deviations less than a 60 mm threshold will have little or no effect on overall jacking forces. Both vertical and horizontal deviations were found to be small (<50 mm and <10 mm respectively) for Drives A and B and will not be considered further in this paper.

3.2 Lubrication volumes

Based on experience of monitoring on numerous pipe-jacking projects, Praetorius and Schöber (2017) recommended that a lubricant volume of 3.12 times the overcut volume (hereafter referred to as lubrication volume ratio) was applied when tunnelling in sands, 2.58 in fine sands and 2.0 in silts. The surplus lubricant seeped into the ground, creating a filter cake serving as a membrane or zone of low permeability to transfer the support pressure acting in the annular gap (assuming it is stable) into the grain structure of the ground (Praetorius & Schöber, 2017).

The variation in lubrication volume ratio with jacked distance is presented in Fig. 7. Beyond a jacked length of 62 m, the volume ratio stabilizes at 6.02–6.66 for Drive A. Values range between 4.16 and 5.03 for Drive B, but there is a steady increase from a jacked distance of ~200 m to the end of the drive. These values are well in excess of recommended minimum values for filter cake formation. The differences in the average τ values from Drives A and B clearly reflect the differences in volume ratios.

The volume percentage of bentonite pumped into the annulus is plotted (on a log scale) against jacked distance in Fig. 8 for a selection of the 21 stations. The distance

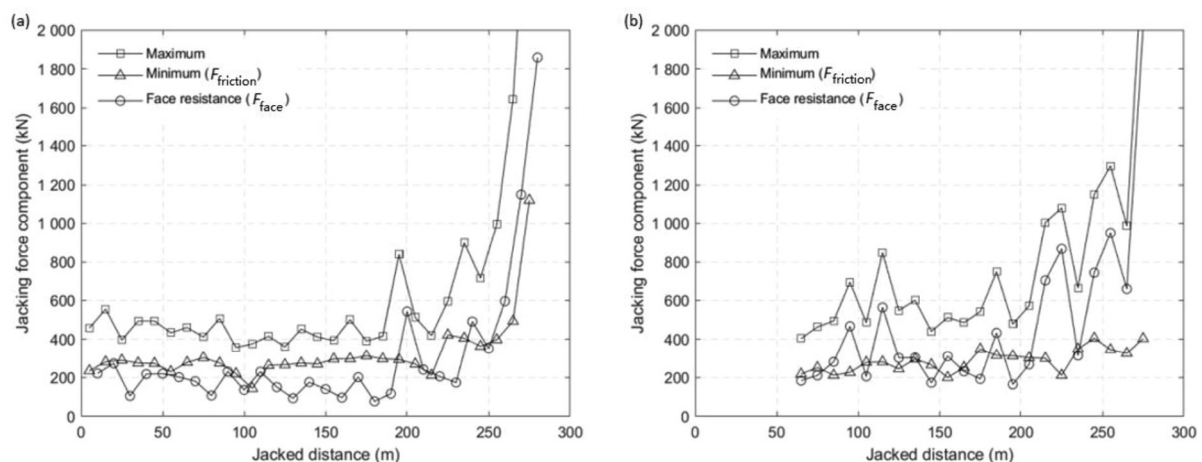


Fig. 4. Maximum and minimum jacking force envelopes and face resistance for (a) Drive A and (b) Drive B.

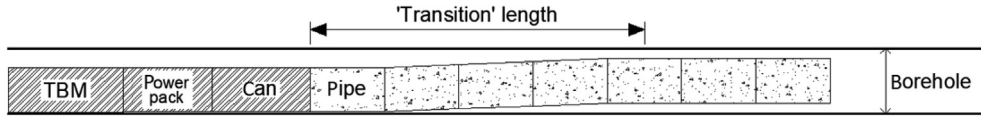


Fig. 5. Hypothesised transition of pipe string within bore.

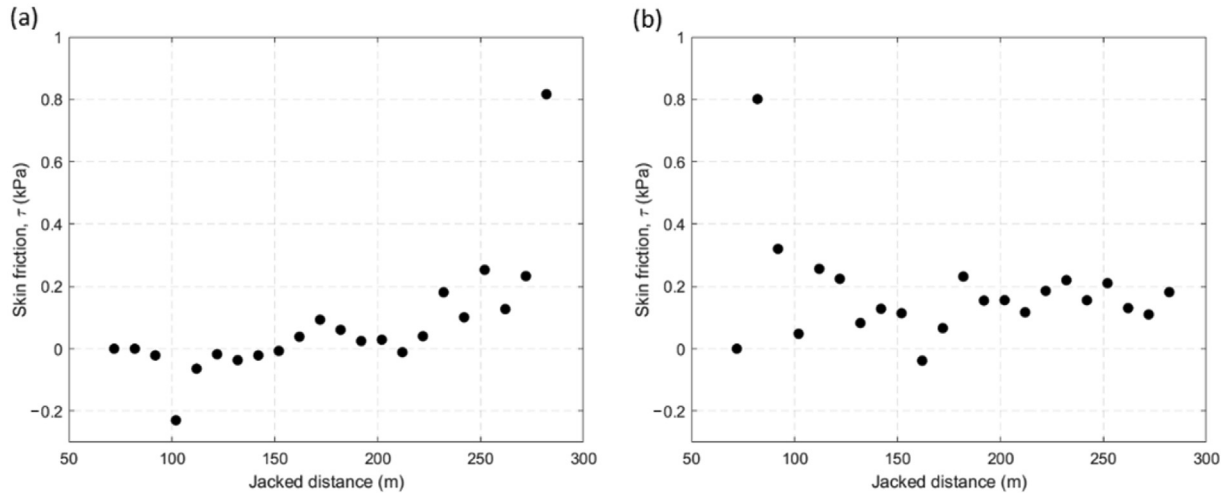


Fig. 6. Average skin friction for (a) Drive A and (b) Drive B.

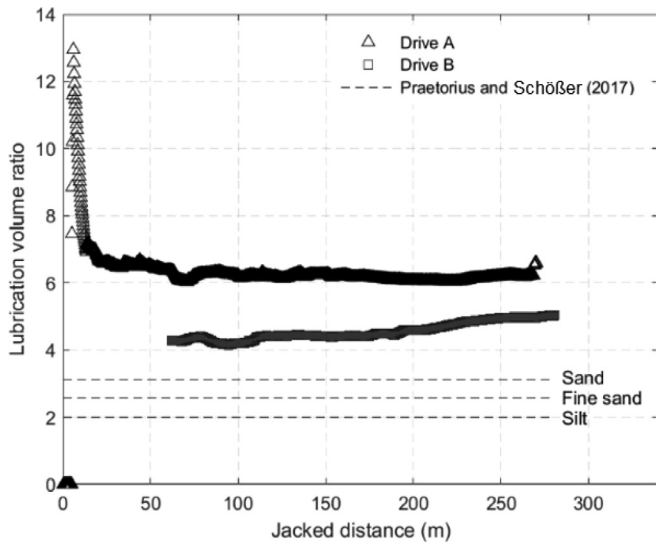


Fig. 7. Normalised bentonite volume against jacked distance for Drives A and B.

of these stations behind the TBM face is shown in the legend. Station 1 (the nearest to the TBM) is responsible for a greater bentonite volume than any other individual station for most of the drive length. The bentonite volume supplied at the head of the machine supports the borehole and it is intended that the trailing pipes maintain a constant lubrication volume ratio thereafter (confirmed in Fig. 7), as over time bentonite may dissipate through the soil. Around the midpoint of Drive A (135 m), for example, Station 1 has produced 44% of the total volume of bentonite, the station located at the launch shaft has

contributed 13% and Stations 2 and 3 supplied 10.9% and 6.4% respectively. Therefore, these four stations contribute 74.3% of the total volume of bentonite at this position.

3.3 Pipe buoyancy

Pipes are generally designed to remain buoyant in a stable lubricated overcut. However, the stability of the overcut in sandy soils is generally a source of uncertainty, therefore the flotation status of the pipe string is generally unknown during installation. The data enable a retrospective assessment of the effective weight (W_{eff}) of the pipe to be made. Making σ'_n the subject of Eq. (1) and recognizing that σ'_n cannot be negative, the following inequality is obtained:

$$\sigma'_n = \frac{\tau}{\tan \delta_p} - \frac{|W_{eff}|}{\pi DL} \geq 0. \quad (2)$$

In terms of a weight ratio W_{eff}/W , the expression can be recast as:

$$\left| \frac{W_{eff}}{W} \right| \leq \frac{\pi DL \tau}{W \tan \delta_p}. \quad (3)$$

Reilly and Orr (2017) conducted direct shear interface tests between a fine to medium sand (median particle size $D_{50} = 0.23$ m) and a rough concrete interface in which 4% and 8% Hydraul-EZ bentonite mixes were used. Interface friction angles of 31° and 27.1° were measured for the 4% and 8% mixes respectively. A value of 28.8° was adopted for δ_p in Eq. (3) based on interpolation of the

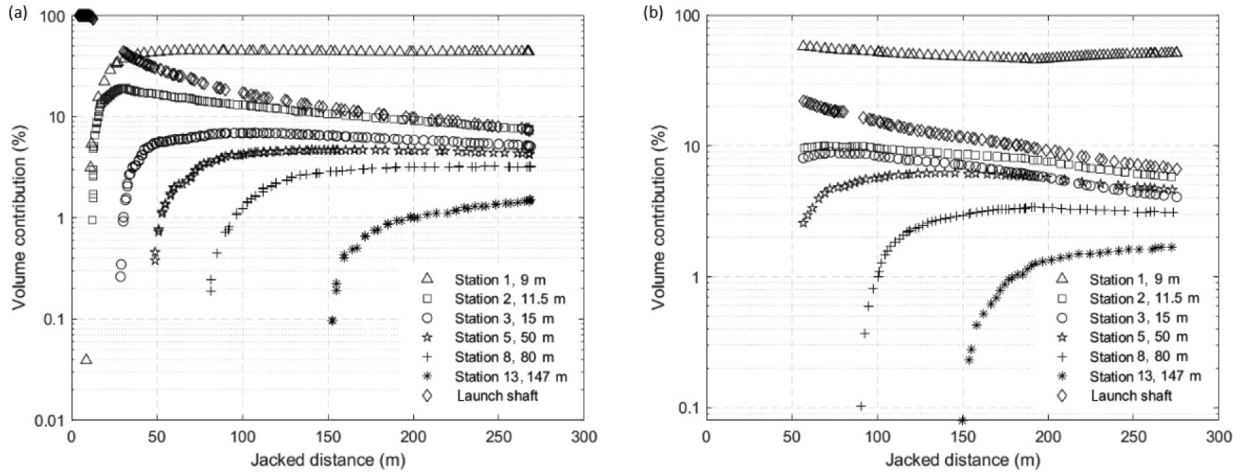


Fig. 8. Percentage of total bentonite volume pumped from selected stations for (a) Drive A and (b) Drive B.

Reilly and Orr (2017) values for the 5.7% mix used at the Blackpool site. Values of W_{eff}/W are plotted against jacked distance for Drives A and B in Fig. 9; note that these represent average values over the length of the pipe string. Values are plotted around full buoyancy ($-0.1 < W_{\text{eff}}/W < 0.1$) for Drive A, with slightly higher values ($0 < W_{\text{eff}}/W < 0.25$) for Drive B where less bentonite was injected. It can therefore be inferred that the pipe train remained relatively central within the bore, a conclusion which is not particularly sensitive to the value of δ_p assumed. Locally high values of W_{eff}/W coincide with the increased τ values associated with stoppages.

3.4 Overcut stability

The integrity of the overcut when pipe-jacking in sandy soils is often unknown. Khazaei, Shimada, Kawai, Yotsumoto, and Matsui (2006) used a camera and ground penetrating radar to consider the integrity of the overcut when tunnelling in sand. Although the surrounding soil had converged slightly on the pipe, it was confirmed that lubrication was present in every sampling area, supporting the possibility of a stable overcut in such soils.

If the hypothesis of an unstable overcut is adopted, σ'_n acting on the pipe crown (assumed equal to σ'_v) may be determined from a number of expressions emanating from Terzaghi (1943) arching theory. Four methods (Terzaghi, 1951; ATV A 161 (Stein, Mollers, & Bielecki, 1989); PJA (Milligan & Norris, 1994) and Zhang, Zhang, Zhou, Dong, & Ma, 2016) were used to calculate σ'_v . The arching geometry parameters H (the cover to the pipe crown), B (the influencing (silo) width of soil above the pipe) and D_b (the bore diameter) are shown in Fig. 10. The method proposed by Terzaghi (1951), based on Eqs. (4) and (5) below, was found to provide the lowest estimate of σ'_v (14.5–15.6 kPa) for the range of covers encountered over both drives (H/B between 3.43 and 5.18); γ' is the effective unit weight, K is the earth pressure coefficient above the pipes, δ is the interface angle along the silo's shear planes and ϕ is the friction angle.

$$\sigma'_v = \gamma' H \left(\frac{1 - e^{-2K \frac{H}{B} \tan \delta}}{2K \frac{H}{B} \tan \delta} \right), \quad (4)$$

$$B = D_b \left(1 + 2 \tan \left(\frac{\pi}{4} - \frac{\phi}{2} \right) \right). \quad (5)$$

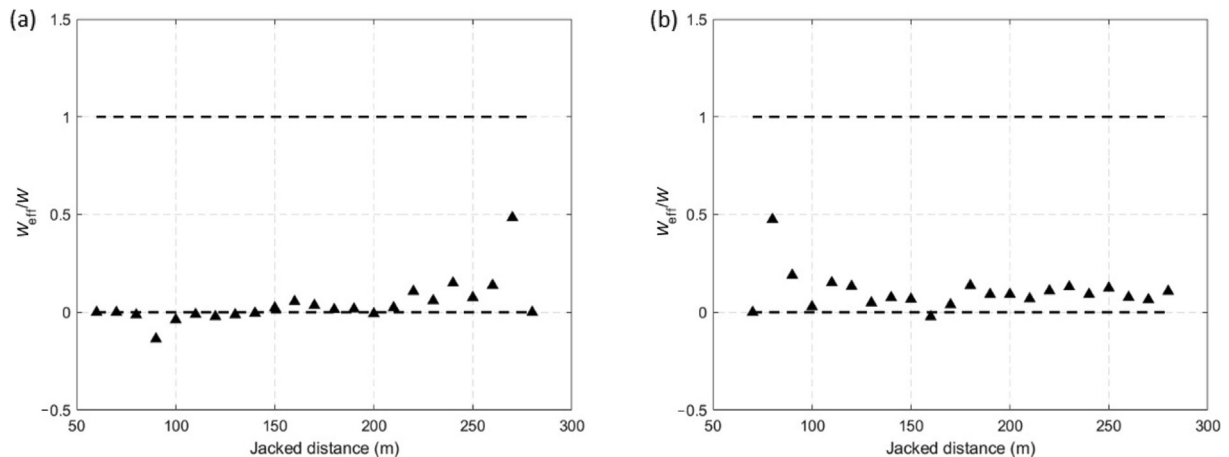


Fig. 9. Values of W_{eff}/W against jacked distance, demonstrating pipe string buoyancy for (a) Drive A and (b) Drive B.

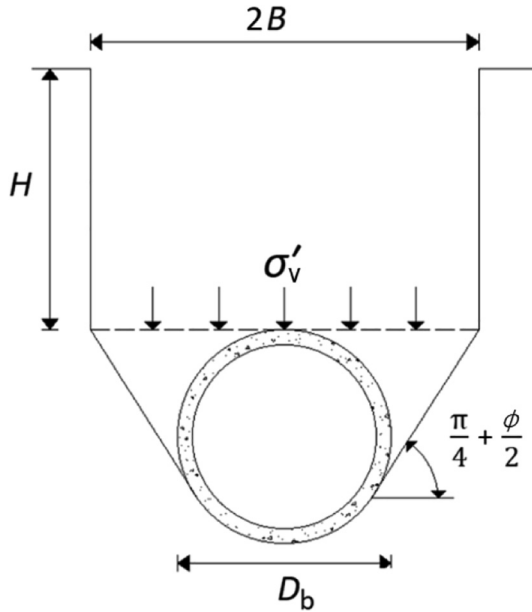


Fig. 10. Silo pipe loading model.

The corresponding frictional stresses, τ , provided by Eq. (1) (9.1–9.7 kPa) are significantly greater than the back-calculated values of τ presented in Fig. 6, rejecting the hypothesis and suggesting that the overcut is in a stable condition.

Furthermore, Atkinson and Potts (1977) developed closed-form analytical solutions for the prediction of the stability of shallow circular tunnels in cohesionless soil using the upper and lower bound theorems of plasticity. The lower bound solution for the support pressure at a state of incipient collapse of the tunnel is defined as follows (Atkinson & Potts, 1977):

$$\sigma_T = \gamma' D \frac{1}{2(\mu - 2)} \left[\left(\frac{1}{2H/D + 1} \right)^{\mu - 2} \left(3 - \frac{4}{\mu} \right) - 1 \right] \leq \gamma' D \frac{\mu}{\mu^2 - 1}, \quad (6)$$

where σ_T is the fluid support pressure in the tunnel annulus, and μ is defined as follows:

$$\mu = \frac{1 + \sin \phi'}{1 - \sin \phi'}. \quad (7)$$

ϕ' is the maximum angle of shearing resistance. The upper bound support pressure is defined as:

$$\sigma_T = \frac{\gamma' D}{4 \cos \phi'} \left(\frac{1}{\tan \phi'} + \phi' - \frac{\pi}{2} \right). \quad (8)$$

For the drives in this paper, values of σ_T are required to maintain stability range between 1.6 kPa and 3.2 kPa for the upper and lower bound calculation respectively. It is highly likely that these pressures have been achieved for these drives given that the average and maximum pressures during lubricant pumping (recorded before entering the pipeline) were 770 kPa and 3.27 MPa respectively.

3.5 Penetration/advance rates

Penetration rate is defined as jacked length per unit jacking time. Average penetration rates for Drives A and B are 121 mm/min and 106 mm/min respectively. These rates fall between the penetration rates quoted by Praetorius and Schöber (2017) for clay (20–80 mm/min) and sand (120–260 mm/min), consistent with the drive being predominantly in silt/silty sand. These exceed the values of 20.6 mm/min and 21.1 mm/min presented by Cui, Xu, Shen, Yin, and Horpibulsuk (2015) for drives straddling silty clay and silty sand.

Advance rates include tunnelling downtime for pipe changes, maintenance and breakdowns (but not overnights), and the utilisation ratio, defined as the ratio of advance rate to penetration rate, may be used as a means of evaluating TBM performance (Alber, 1996). The latter parameter is typically related to the cutter head wear in rock drives, and as such, there is little such data with which to compare for silty/sandy soils. The utilisation ratio is itemised for each day for both Drives A and B in Fig. 11, with average values of ~31% for both drives. Assuming 24 h shifts (not explicitly stated in their paper), similar values (38% and 46%) were inferred for the Cui et al. (2015) drives.

3.6 Stoppages

Localised peaks in jacking force arise as a result of stoppages in tunnelling, such as pipe changes, maintenance, overnights and weekends. A zoomed-in example of such jacking force peaks and subsequent decay to baseline force values for Drive A is shown in Fig. 12.

All individual stoppages arising in Drives A and B are represented on a plot of increase in jacking force against jacked distance (Fig. 13). The jacking force increase is calculated as the initial force after a stoppage minus the force immediately before the stoppage. Stoppages are categorized according to duration (t) as follows for Drive A: $t < 30$ min for pipe changes only; $30 \text{ min} < t < 2$ h for breaks and daily (line) checks, which may also include pipe changes; $2 \text{ h} < t < 5$ h due to maintenance and minor issues, which may also include pipe changes; $12 \text{ h} < t < 20$ h for overnight stoppages and $t > 20$ h for weekends. Slightly different categories are used for Drive B; since there were no stoppages between 3 h and 5 h, a time category of $30 \text{ min} < t < 3$ h was used. The negative values of jacking force registered on Fig. 13 are likely to represent a more conservative driving style upon commencement of jacking, and have been ignored for the purposes of determining the best fit lines for each time category on Fig. 13. The corresponding frictional stress increases (i.e. related to the slopes of the lines in Fig. 13) are plotted for each time category on Fig. 14 (the marker denotes the midpoint of the time range, which is denoted by the range bars).

From Figs. 13 and 14, the following conclusions can be drawn:

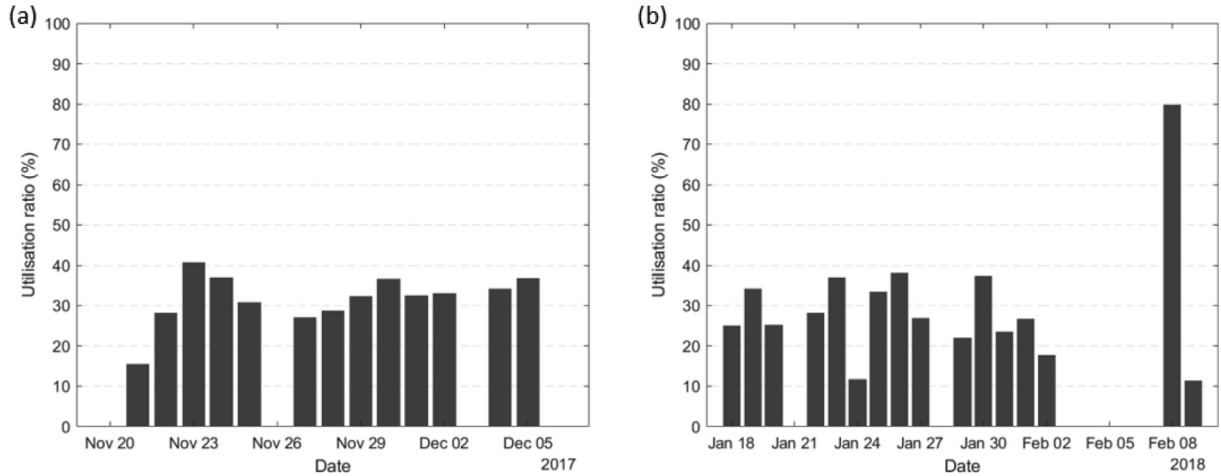


Fig. 11. Utilisation ratios for each day for (a) Drive A and (b) Drive B.

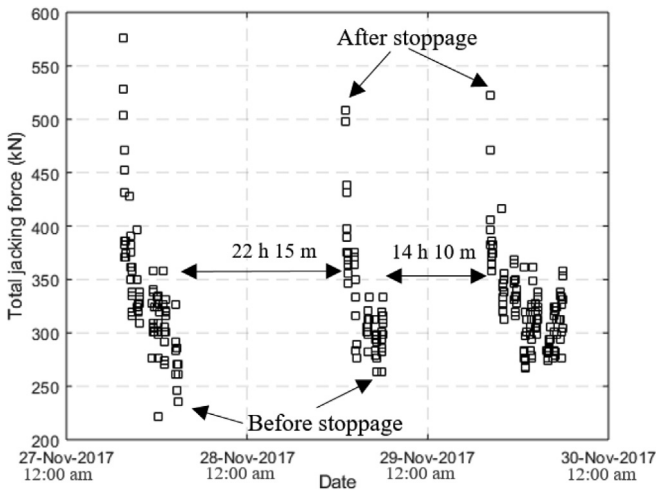


Fig. 12. Influence of stoppages on total jacking force (Drive A).

- (1) The jacking force increase required after a stoppage depends on jacked length, confirming that it is a frictional phenomenon.

- (2) The duration of stoppage has little effect on the jacking force required up to about 2–3 h (frictional stress increase less than 0.05 kPa), but it has a clear effect for longer durations. This observation would appear to rule out differences in static and dynamic coefficients of friction as the explanation for the frictional stress increases.
- (3) There are two best fit lines shown for the 12–20 h category for Drive B. The reduced jacking forces beyond ~200 m may reflect the increase in lubrication volume ratio from that point until the end of the drive. Interestingly, this effect was not observed for the lower stoppage duration categories.
- (4) In Fig. 14, the effect of lubrication volume ratio is apparent, where frictional stress increases are higher for Drive B than Drive A for the longer stoppages.
- (5) Stoppages greater than 20 h are of significant concern with increases of 0.31 kPa and 0.5 kPa for Drive A and B respectively, much greater than the average skin friction values for these drives.

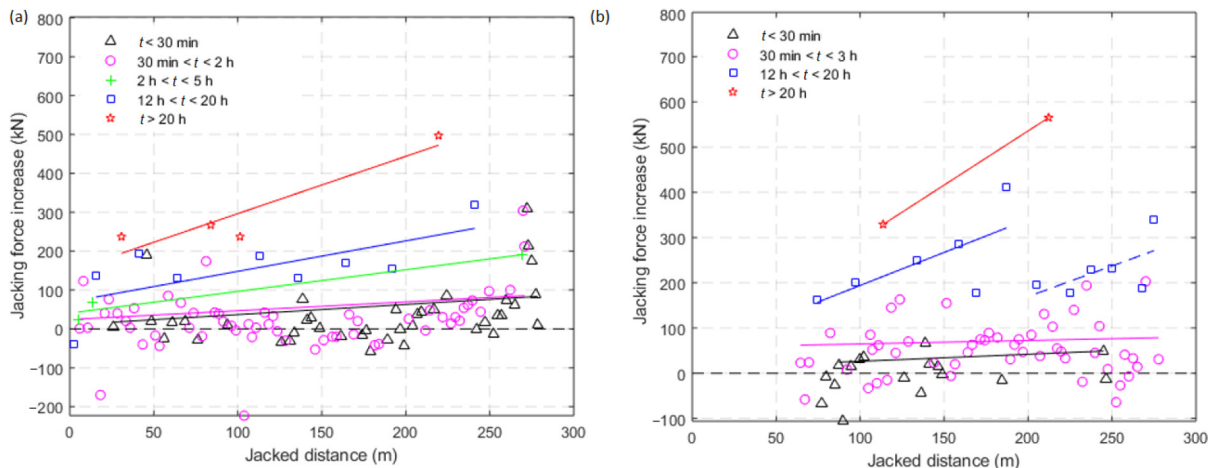


Fig. 13. Change in jacking force due to stoppage against jacked distance for (a) Drive A and (b) Drive B.

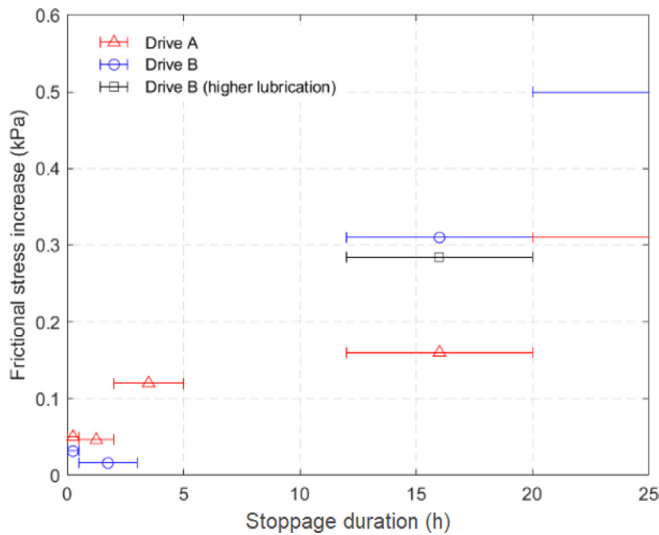


Fig. 14. Relationship between frictional stress increase and stoppage duration.

4 Conclusions

Data from two 1 200 mm internal diameter microtunnels installed through silt and silty sand are interpreted in this paper. The following conclusions and research questions prompted as a result can be summarized:

- (1) The strategy of deploying lubrication volume ratios much greater than the Praetorius and Schöber (2017) guideline values was justified by the very low average skin friction values (less than 0.5 kPa) for the pipe string. Slightly different values for the two drives reflect slightly different lubrication volume ratios. The relationship between average skin friction and lubrication volume ratio is a topic worthy of systematic research at field scale.
- (2) The skin friction values for the pipe string were used to infer that the pipe string is on average fully buoyant in a stable annulus based on normal effective stresses calculated from arching models and drained tunnel stability theory. However, a robustly-instrumented pipe capable of measuring normal and shear stresses would provide important localized insight into the behaviour of the annulus.
- (3) The increase in frictional stress owing to stoppages is strongly time dependent, at least beyond about 2–3 h, and also reflects the amount of bentonite injected. The frictional stress increases associated with longer stoppages are multiples of the steady state values. The time effect would suggest that one of the theories put forward for this frictional stress increase, different coefficients of static and dynamic friction, is improbable. Sensors positioned to record external bentonite

pressures (in an open or collapsed annulus) would aid in understanding the mechanism behind such frictional stress increases.

A secondary goal of this paper is to highlight the usefulness of retrospective analysis of drive data, which is largely untapped by the pipe-jacking industry. The potential for new understanding of the pipe-jacking process by collating experiences of drives in different ground conditions, particularly in the context of modern data analytics capability, is very exciting.

Acknowledgements

The first author is funded by an Irish Research Council Enterprise Partnership Scheme (IRC-EPS) Postgraduate Scholarship, with Ward and Burke Construction Limited as the industry partner. The third author is supported by the Royal Academy of Engineering (U.K.) under the Research Fellowship Scheme.

References

- Atkinson, J. H., & Potts, D. M. (1977). Stability of a shallow circular tunnel in cohesionless soil. *Géotechnique*, 27(2), 203–215.
- Alber, M. (1996). Prediction of penetration, utilization for hard rock TBMs. In Proceedings of the international conference of Eurock '96, Balkema, Rotterdam (pp. 721–725).
- Borghi, F. X. (2006). *Soil conditioning for pipe-jacking and tunnelling*. PhD thesis. UK: University of Cambridge.
- Barla, M., & Camusso, M. (2013). A method to design microtunnelling installations in randomly cemented Torino alluvial soil. *Tunnelling and Underground Space Technology*, 33, 73–81.
- Chapman, D. N., & Ichioka, Y. (1999). Predictions of jacking forces for microtunnelling operations. *Tunnelling and Underground Space Technology*, 14(1), 31–41.
- Cheng, W., Ni, J. C., Shen, J. S., & Huang, H. (2017). Investigation into factors affecting jacking force: A case study. *Proceedings of the Institution of Civil Engineers – Geotechnical Engineering*, 170(4), 322–334.
- Cheng, W., Ni, J. C., Arulrajah, A., & Huang, H. (2018). A simple approach for characterising tunnel bore conditions based upon pipe-jacking data. *Tunnelling and Underground Space Technology*, 71, 494–504.
- Cui, Q. L., Xu, Y. S., Shen, S. L., Yin, Z. Y., & Horpibulsuk, S. (2015). Field performance of concrete pipes during jacking in cemented sandy silt. *Tunnelling and Underground Space Technology*, 49, 336–344.
- Curran, B. G., & McCabe, B. A. (2011). Measured jacking forces during slurry-shield microtunnelling in a boulder clay at Kilcock, Ireland. In Proceedings of the 15th European conference on soil mechanics and geotechnical engineering, Athens (Vol. 3, pp. 1627–1632).
- Khazaei, S., Shimada, H., Kawai, T., Yotsumoto, J., & Matsui, K. (2006). Monitoring of over cutting area and lubrication distribution in a large slurry pipe jacking operation. *Geotechnical and Geological Engineering*, 24(3), 735–755.
- Marshall, M. (1998). *Pipe-jacked tunnelling: Jacking loads and ground movements*. PhD Thesis. UK: University of Oxford.
- McGillivray, C. B., & Frost, J. D. (2010). Influence of bentonite slurry on interface friction. In *Characterization and behaviour of interfaces – Proceedings of research symposium on characterization and behaviour of interfaces* (pp. 119–124). Atlanta: IOS Press.
- Milligan, G., & Norris, P. (1994). *Pipe jacking research results and recommendations*. (p. 18).
- Ni, J. C., Ge, L., & Cheng, W. (2016). Variation of slurry pipe jacking on coarse and fine soils. In 4th GeoChina international conference

- sustainable civil infrastructures: Innovative technologies for severe weathers and climate changes.
- Pellet-Beaucour, A. L., & Kastner, R. (2002). Experimental and analytical study of friction forces during microtunnelling operations. *Tunnelling and Underground Space Technology*, 17(1), 83–97.
- Praetorius, S., & Schöber, B. (2017). *Bentonite handbook: Lubrication for pipe jacking*. John Wiley and Sons.
- Reilly, C. C. (2014). *The influence of lubricant slurries on skin friction resistance in pipe jacking*. PhD thesis. Trinity College Dublin.
- Reilly, C. C., McCabe, B. A., & Orr, T. L. L. (2012). Analysis of microtunnel jacking forces in alluvium and glacial till in Mullingar, Ireland. World Tunnelling Conference, Bangkok.
- Reilly, C. C., & Orr, T. L. L. (2012). Analysis of interface friction effects on microtunnel jacking forces in coarse-grained soils. In *Proceedings of the bridge and concrete research in Ireland Conference, Dublin* (pp. 121–126).
- Reilly, C. C., & Orr, T. L. L. (2017). Physical modelling of the effect of lubricants in pipe-jacking. *Tunnelling and Underground Space Technology*, 63, 44–53.
- Sheil, B. B., Curran, B. G., & McCabe, B. A. (2016). Experiences of utility microtunnelling in Irish limestone, mudstone and sandstone rock. *Tunnelling and Underground Space Technology*, 51, 326–337.
- Shou, K., Yen, J., & Liu, M. (2010). On the frictional property of lubricants and its impact on jacking force and soil-pipe interaction of pipe-jacking. *Tunnelling and Underground Space Technology*, 25, 469–477.
- Staheli, K. (2006). *Jacking force prediction: an interface friction approach based on pipe surface roughness*. PhD Thesis. Georgia Institute of Technology, USA.
- Stein, D., Möllers, K., & Bielecki, R. (1989). *Microtunneling*. (p. 352).
- Stroud, M. A. (1989). The Standard Penetration Test – its application and interpretation. In *Proceedings of the ICE conference on penetration testing in the UK*, Thomas Telford, London.
- Terzaghi, K. (1943). *Theoretical soil mechanics*. New York: Wiley and Sons.
- Terzaghi, K. (1951). *Mécanique des sols*. (pp. 188–474).
- Ulkan, A. (2013). Development in trenchless technologies at Herrenknecht. GSTT 1st No Dig Berlin 2013, Berlin (pp. 2A-1-1–2A-1-6).
- Zhang, H., Zhang, P., Zhou, W., Dong, S., & Ma, B. (2016). A new model to predict soil pressure acting on deep burial jacked pipes. *Tunnelling and Underground Space Technology*, 60, 183–196.
- Zhang, P., Behbahani, S. S., Ma, B., Iseley, T., & Tan, L. (2018). A jacking force study of curved steel pipe roof in Gongbei tunnel: Calculation review and monitoring data analysis. *Tunnelling and Underground Space Technology*, 72, 305–322.